Altitude and Latitude Dependence of Bursts in a Lead-Shielded Ionization Chamber*

ALLEN J. MCMAHON, BRUNO ROSSI,** AND W. F. BURDITT
Brookhaven National Laboratory, Upton, New York
(Received June 19, 1950)

The instrument used in this experiment consisted of a cylindrical ionization chamber covered by a half-cylindrical 15-cm thick lead (Pb) shell. Five trays of G-M tubes were placed around the shell and one tray directly below the ionization chamber. Various kinds of coincidences were recorded between bursts of ionization in the chamber and discharges of the G-M tubes. This equipment was flown in a B-29 at Rome, New York (geomagnetic latitude 55°N), and at Panama (geomagnetic latitude 20°N). The experiment provided information on the altitude, latitude, and angular dependence of the radiation responsible for the observed events. These were interpreted as due to nuclear interactions by nucleons of different energies. In particular, for events attributed to protons with an estimated minimum energy of about 5 Bev the intensity ratio between 55°N and 20°N at 30,500 feet was 1.17 ± 0.04. In contrast, for events attributed to protons with an estimated minimum energy of about 0.4 Bev the latitude ratio at the same altitude was 1.96 ± 0.18.

I. INTRODUCTION

THE work of Bridge, Rossi, and Williams[1] has shown that the observation of bursts in a shielded ionization chamber occurring in coincidence with discharges in trays of G-M tubes provides a convenient method for the detection of nuclear interactions of cosmic rays. This method was used by the authors mentioned above as well as by other experimenters[2–7] for the investigation of the dependence on altitude or depth and the absorption in various materials of the particles responsible for the nuclear interactions. The present experiment is designed to provide information on the latitude and angular dependence of these particles as well as to check the previous data on their variation with altitude.

II. EXPERIMENTAL ARRANGEMENT

The arrangement of the ionization chamber, G-M tubes and absorber is shown in Fig. 1. The ionization chamber (I) had a diameter of 7.5 cm and an effective length of 52 cm. It had copper walls $\frac{1}{32}$ in. thick (0.7 g cm^{-2}) and was surrounded by a $\frac{1}{4}$-in. (0.64 g cm^{-2}) Lucite electrical insulator. It was filled with pure argon at 4.0 atmos. pressure above vacuum (at 25°C) and it contained a polonium source of alpha-particles at the inner surface of the cylindrical wall. The pulses produced by the polonium alpha-particles (5.3 Mev) served as a standard for the measurement of the ionization bursts observed in the chamber. The size of these pulses will be designated as P_α. A pulse of this size corresponds to the amount of ionization produced by the passage through the chamber of about 100 electrons of 10 Mev traveling perpendicularly to the chamber axis.[4]

Each of the G-M tubes was 2.5 cm in diameter and had an effective length of 50 cm. These tubes were arranged in six trays, five trays consisting of five tubes (A), and one tray of four tubes (B). All tubes in any one tray were connected in parallel. The five trays A were placed above the lead absorber (Pb) and tray B was placed below the ion chamber in a tunnel in the absorber. The total amount of material between the sensitive volume of the ion chamber and of the G-M tubes B was about 2 g cm^{-2}. The lead absorber (Pb) separating the chamber from the upper trays A was 5 cm thick and it extended 9 cm beyond the sensitive volume of the chamber on each end.

The ion chamber pulses were amplified by a Los Alamos Model 100 amplifier and passed through a pulse-height discriminator selecting pulses greater than $0.6P_\alpha$. Coincidences between these pulses and a discharge of any one of the six G-M trays were selected by a circuit with about 15 μsec. resolving time and made to operate the horizontal sweep of an oscilloscope. The pulses of the chamber, properly delayed, were applied

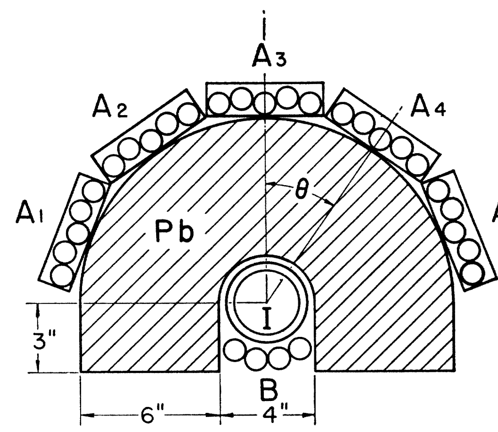

FIG. 1. Experimental arrangement; ionization chamber, Geiger-Müller tubes and absorber.

* Research carried out at Brookhaven National Laboratory under auspices of the AEC.
** At Massachusetts Institute of Technology, Cambridge, Massachusetts.
[1] Bridge, Rossi, and Williams, Phys. Rev. **72**, 257 (1947).
[2] E. P. George, Nature **160**, 327 (1947).
[3] Bridge, Hazen, Rossi, and Williams, Phys. Rev. **74**, 1083 (1948).
[4] H. Bridge and B. Rossi, Phys. Rev. **75**, 810 (1949).
[5] E. F. Fahy and M. Schein, Phys. Rev. **75**, 207 (1949).
[6] D. Hudson, Cornell thesis (1950).
[7] R. H. Rediker, M.I.T. thesis (1950).

to the vertical deflecting plates of this oscilloscope, whose screen was photographed on a continuously moving film. A record of the trays which had been discharged in coincidence with pulses of the ion chamber was obtained on this same film. This was done by means of neon bulbs which were turned off in the event of a coincident discharge of a tray and of the ion chamber. To supplement the photographic record, electronically driven registers recorded the total number of chamber pulses greater than $0.6P_\alpha$, and the total number of coincidences between these pulses and any of the G-M trays. A scaling circuit driving a third register could be connected to the separate trays of G-M tubes to determine their counting rates.

Bias curves of the alpha-particle pulses were measured periodically and served as a primary calibration for the setting of the discriminator. An electronic pulser was used as a secondary standard to record

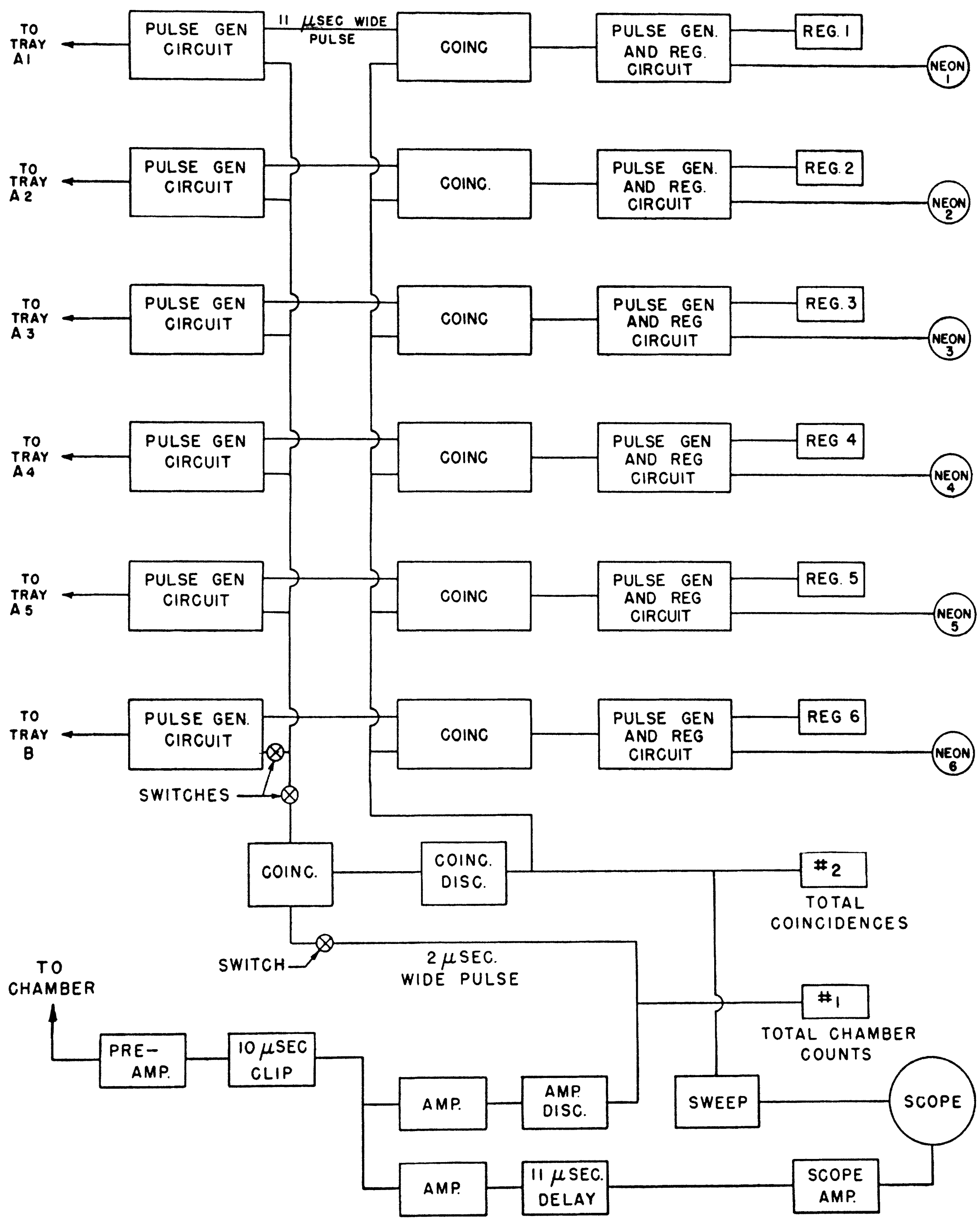

FIG. 2. Block diagram of the electronic circuits.

TABLE I. Counting rates per minute at various altitudes and latitudes. (Errors are standard statistical deviations.)

Atmospheric depth g cm⁻²	Time (min.)	*AIB* Uncorr.	*AIB* Corrected	*AI–B* Uncorr.	*AI–B* Corrected	*IB–A* Uncorr.	*IB–A* Corrected	Remarks
Geomagnetic latitude 55°N								
383	582	1.23	1.21 ±0.05	0.72	0.465±0.04	1.11	1.13±0.04	4 flights May '49
300	180	2.39	2.33 ±0.11	1.17	0.91 ±0.09	1.85	1.91±0.10	1 flights Sept. '49
273	285	3.00	2.92 ±0.10	1.66	1.102±0.09	2.41	2.47±0.09	3 flights May '49
Geomagnetic latitude 20°N								
383	422	1.10	1.085±0.05	0.46	0.301±0.04	0.85	0.86±0.04	3 flights June '49
300	324	2.10	2.11 ±0.08	0.65	0.423±0.06	1.65	1.68±0.07	2 flights June '49
300	388	1.93	1.90 ±0.07	0.61	0.480±0.04	1.40	1.43±0.06	3 flights Sept. '49

pulses of known size on each film. The bias curves showed a flat plateau followed by a very steep drop indicating a spread of less than four percent in the size of the alpha-particle pulses. The gain of the amplifier was constant to better than two percent over the whole series of measurements.

A complete self-explanatory block diagram of the electronic circuits is shown in Fig. 2.

The equipment was installed in the rear pressure cabin of a B-29 airplane. At all times the axis of the chamber was perpendicular to the direction of flight.

III. EXPERIMENTAL RESULTS

Measurements were made with the airplane flying both in the east and in the west directions along geomagnetic parallels at 55°N and at 20°N geomagnetic latitude. For the flights at 55°N the plane was based at Rome, New York and for the flights at 20°N at Panama. From both bases, flights were made at 30,500 feet (300 g cm^{-2} atmospheric depth) and at 25,000 feet (383 g cm^{-2}). In addition, some flights were made at 32,500 feet (273 g cm^{-2}) from Rome, New York.

Table I lists the experimental results concerning three types of events which we shall designate as *AIB*, *AI–B*, and *IB–A*. The *AIB* event is a threefold coincidence between a discharge of trays *A*, a discharge of tray *B*, and a pulse larger than $0.6P_\alpha$ in the ionization chamber *I*. An *AI–B* event is a double coincidence between a discharge of tray *A* and a pulse greater than $0.6P_\alpha$ in *I* not accompanied by a pulse in tray *B*. An *IB–A* event is a double coincidence between a pulse greater than $0.6\,P_\alpha$ in *I* and the discharge of tray *B* not accompanied by a pulse in an upper tray *A*.

As is indicated in Table I, several flights were made at each altitude and latitude. The data from the different flights were consistent with one another within the experimental errors, except for some of those obtained during two groups of flights made at 20°N and 300 g cm^{-2} in June and in September, 1949, respectively. For this reason the results of these two groups of flights are shown separately in Table I. Since there is no objective ground on which to reject either one of the two experiments, we shall use the weighted averages of their results in our discussion.

During some of the flights at 55°N and 383 g cm^{-2} tray A_5 was removed from its normal position and placed horizontally with its center 184 cm from the chamber axis in order to test the effect of air showers. In a total of 300 minutes observation time, tray A_5 was discharged only four times in coincidence with the ion chamber and the lower tray *B*. This shows that only a negligible number of the events recorded by our arrangement can be due to air showers. The counting rates observed during the time that tray A_5 was displaced were, of course, corrected for the consequent decrease in the detection efficiency of the equipment.

Table I lists the observed counting rates as well as the counting rates corrected for accidentals. Accidentals include: (1) Chance coincidences between *AI* coincidences and unrelated *B* discharges; these turn out to be negligible. (2) Chance coincidences between *IB* coincidences and unrelated *A* discharges; these tend to increase slightly the *AIB* rate and correspondingly to decrease the *IB–A* rate. (3) Chance coincidences between discharges of the counter trays and uncorrelated pulses in the ion chamber. Most of these are due to the presence of the polonium source within the chamber, and their number decreases with time because of the decay of the polonium source (138.3-day half-life).[8] Such events increase the *AI–B* rate considerably and the *IB–A* rate very slightly. (4) Chance coincidences between *AB* coincidences and uncorrelated ion chamber

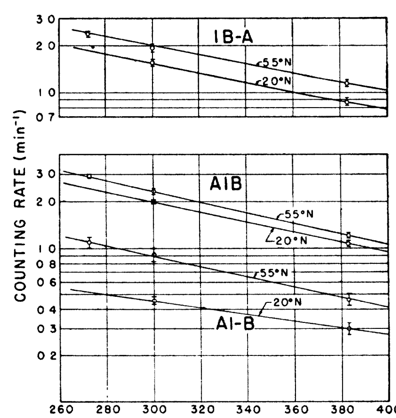

FIG. 3. Counting rates *vs.* atmospheric depth.

[8] W. H. Beamer and W. E. Easton, J. Chem. Phys. 17, 1300 (1949).

TABLE II. Absorption thicknesses (L) and latitude effects. (Errors are standard statistical deviations.)

	Event		
	AIB	*AI–B*	*IB–A*
$L-55°N$	125 ± 8 (g cm^{-2})	127 ± 30 (g cm^{-2})	143 ± 10 (g cm^{-2})
$L-20°N$	135 ± 11 (g cm^{-2})	198 ± 50 (g cm^{-2})	143 ± 11 (g cm^{-2})
$N_{55°}/N_{20°}$(300 g cm^{-2})	1.17 ± 0.04	1.96 ± 0.18	1.32 ± 0.05

pulses; these result in a very slight increase of the *AIB* rate. One sees from Table I that the correction for accidentals is only important in the case of *AI–B* events. Because of this large correction, the experimental results concerning *AI–B* events are less reliable than those concerning either *AIB* or *IB–A* events.

In Fig. 3 the corrected counting rates listed in Table I are plotted on a logarithmic scale against atmospheric depth. The data obtained at 55°N are consistent with an exponential variation of the counting rate with depth. Least-square adjustments of this data to an exponential function of the form const.$\times\exp(-x/L)$ gives for L the values listed in Table II. The same table lists the values of the absorption thicknesses L at 20°N computed from the measurements at 300 g cm^{-2} and at 383 g cm^{-2} under the assumption of an exponential variation with depth. The ratios listed in the last line of Table II represent the latitude effect between 55°N and 20°N for the particles giving rise to *AIB*, *AI–B*, and *IB–A* events at 300 g cm^{-2}. The counting rates at 55°N were obtained from the least-square analysis and those at 20°N from direct measurement.

The pulses of the ion chamber show a variety of shapes corresponding to the different distribution of the ionization in the chamber. Following Bridge *et al.*[3] we have subdivided the pulses into three groups designated respectively as α, σ, and ν. Figure 4 shows sections of a typical record containing examples of the three different pulse shapes. A pulse is classified as an α-pulse if its height at one-half rise time is less than one-third the final height. All other smoothly rising pulses are classified as σ-pulses. Pulses showing discontinuous changes in slope are classified as ν-pulses. We refer to the paper by Bridge *et al.*[3] for a detailed interpretation of these pulse shapes. We wish to point out, however, that the classification of pulse shapes is by necessity somewhat arbitrary, and that the criterion adopted here may not coincide exactly with that adopted by other observers. Pulse shape analysis was made on some of the photographic records and Table III shows the results. The numbers listed in this table give the percent of pulses of different shapes computed after subtracting accidentals. The accidental correction is important only in the case of *AI–B* events where it is due mainly to the background of polonium particles. Background pulses resulting from polonium α-particles have shapes of the type called α in our classification. Of course, we took this into account in distributing the accidental corrections among pulses of different shapes.

The *AIB* events observed at 55°N during the flights at 273 g cm^{-2} and the *AIB* events observed at 20°N during part of the flights at 300 g cm^{-2} were analyzed for pulse height from the photographic records. The results obtained at the two latitudes are not significantly different. They are shown in Fig. 5 in the form of integral pulse-height distributions.

The records obtained at 55°N and most of those obtained at 20°N were also analyzed for single or multiple discharges of the A trays. The results obtained at the two latitudes and at the various altitudes were not significantly different. They are presented together in Fig. 6. The histograms in this figure give the total number of *AIB* and *AI–B* events in which one, two, three, four, or all five trays A were discharged. The data are corrected for accidentals, whose rate is appreciable only for events corresponding to single discharges of the A trays.

Events *AIB* and *AI–B* involving the discharge of only one of the A trays were sorted out according to which of these trays had been discharged in an attempt to study the angular dependence of the radiation responsible for the observed events. The results of this analysis are shown in Fig. 7 in which θ indicates the zenith angle of the line connecting the center of the ion chamber with the center of the tray. The points plotted at $\theta=0(\cos\theta=1)$ are the counting rates of events involving the discharge of tray A_3. The points plotted at

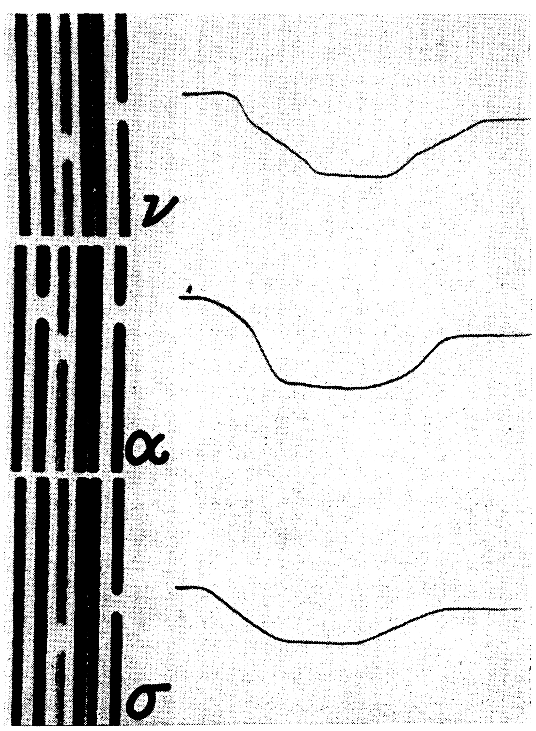

FIG. 4. Samples of photographic records showing a ν-pulse, an α-pulse, and a σ-pulse. The black lines on the left-hand side represent the images on continuous moving film of the neon bulbs recording discharges of the counter trays.

$\theta=35°(\cos\theta=0.82)$ are the averages of the counting rates for events involving trays A_2 and A_4. The points plotted at $\theta=70°(\cos\theta=0.342)$ are the averages of the counting rates for events involving trays A_1 and A_5. In the plane perpendicular to the axis of the chamber each tray subtends an angle of 32°. As an indication of the resolution of the instrument, horizontal lines are drawn through each experimental point to cover this angular interval. As shown by the solid lines, the experimental results are consistent with angular distributions of the $\cos^n\theta$-type. The significance of the dotted lines in the graphs shall be discussed later.

Lastly, we have analyzed the data for east-west asymmetry of the *AIB* and of the *AI–B* events. As noted above, the equipment was flown so that the axis of the chamber always pointed in the N–S direction. For each group of flights we have added together all events involving a discharge in one or both of the two *A* trays facing westward and all events involving a discharge in one or both of the two *A* trays facing eastward. From the numbers, N_W and N_E, thus obtained we have computed the E–W asymmetry, R, by means of the equation:

$$R=2(N_W-N_E)/(N_W+N_E).$$

The results are shown in Table IV. Note that the plane was flown for approximately equal times with trays A_1 and A_2 facing east and with trays A_4 and A_5 facing east, so as to minimize any possible error due to unequal efficiency of the G-M trays.

IV. DISCUSSION

AIB coincidences may be caused by electromagnetic interactions of high energy μ-mesons (knock-on showers, radiation showers), by nuclear interactions of high energy nucleons, or possibly by nuclear interactions of π-mesons. Previous experiments[1,4] have shown that the contribution of μ-mesons is important only near sea level. On the other hand, the number of π-mesons in the atmosphere is probably small compared with that of nucleons because of the very short mean life of π-mesons. One is thus justified in assuming that the events *AIB* observed in the present experiment are produced mainly by high energy protons and, to a considerably smaller extent, by high energy neutrons (in the latter case tray *A* is discharged by secondary ionizing particles ejected in the backward direction; see below).

Nuclear interactions of protons of several hundred Mev energy give rise mainly to stars of heavily ionizing particles (low energy protons and heavier nuclear fragments). Nuclear interactions of protons of greater energies produce heavily ionizing fragments and in addition showers of lightly ionizing particles. These are mainly electron showers initiated by photons arising from the nuclear interactions; they also contain relativistic mesons and protons. Individual heavily ionizing

TABLE III. Percent of pulses of α, σ, and ν shape.

Event	Time (min.)	Pulse shape α	σ	ν
		55°N, 300 g cm⁻²		
AIB	180	16.6	77.0	6.4
AI–B	180	50.3	38.0	11.7
IB–A	180	33.1	60.2	6.7
		20°N, 300 g cm⁻²		
AIB	120	26.8	67.9	5.3
AI–B	324	63.0	31.5	5.5
IB–A	324	32.2	59.8	8.0

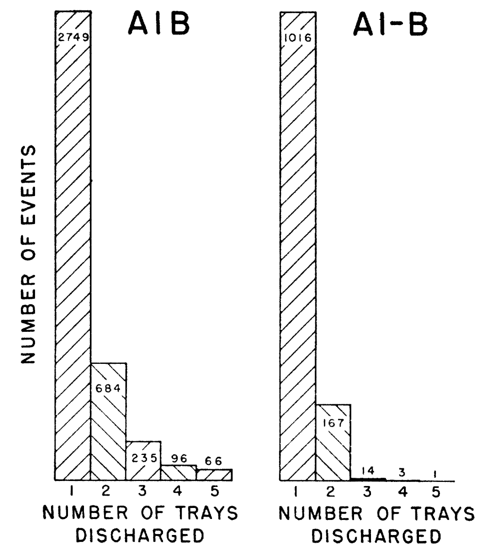

FIG. 6. Distribution of *AIB* and *AI–B* events according to numbers of *A* trays discharged. Data obtained at various latitudes and altitudes are included in this analysis.

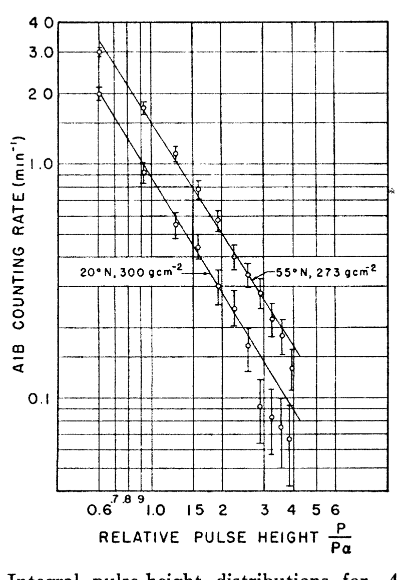

FIG. 5. Integral pulse-height distributions for *AIB* events observed at 55°N, 273 g cm⁻² and at 20°N, 300 g cm⁻². The ordinates represent the counting rates for pulses greater than the corresponding abscissa.

TABLE IV. East-west effect: $R=[2(N_W-N_E)/(N_W+N_E)]$. (Errors are standard statistical deviations.)

	(AIB)	$(AI-B)$
55°N, 273 g cm^{-2}	$R=-0.25\pm0.11$	$R=-0.20\pm0.15$
20°N, 300 g cm^{-2}	$R=+0.10\pm0.10$	$R=+0.20\pm0.16$

particles as well as showers of lightly ionizing particles can produce detectable pulses in the ionization chamber. In the case of an AIB event the requirement of a discharge in tray B rules out nuclear interactions in which only short range, heavily ionizing particles are produced, and thereby discriminates in favor of high energy events. Indeed pulse shape analysis shows that most of the pulses corresponding to AIB events are of the σ-type (see Table III). A σ-pulse corresponds to a fairly uniform distribution of the ionization in the chamber, such as may be produced by a shower of many lightly ionizing particles. We thus conclude that AIB events are mainly due to protons traversing one of the upper A trays and then undergoing a nuclear interaction from which showers of lightly ionizing particles originate. In all likelihood most of these interactions occur in the last few radiation lengths of the lead absorber. A shower capable of giving a pulse of the required size must contain about 60 lightly ionizing particles or more. If such a shower is initiated by a high energy photon the energy of this photon must be at least 5 Bev. The existence of a heavily ionizing particle among the shower particles may lower this limit in individual cases. There is little doubt, however, that in most of the nuclear interactions recorded by the AIB coincidences the energy release is greater than 5 Bev. If the ionization pulses corresponding to AIB events are due mainly to electron showers, their number *vs.* size distribution is representative of the energy distribution of the photons arising from nuclear interactions.[4] As shown in Fig. 5 our experimental results are consistent with an integral pulse-height distribution represented by a power law with an exponent equal to about -1.60. This may be compared with the results of a similar experiment by Bridge and Rossi[4] giving the integral pulse-height distribution as a power law with exponent -1.55.

Events in which tray B fails to be discharged ($AI-B$ events) must be due mainly to protons either entering the ionization chamber near the end of their range or producing stars whose heavily ionizing products traverse the chamber but fail to penetrate counters B. This is confirmed by the pulse shape analysis showing that more than one-half of the pulses corresponding to $AI-B$ events are of the α or ν-type (see Table III). Pulses of these types correspond to a concentrated ionization such as is produced by a single or several heavily ionizing particles. Protons which enter the ionization chamber near the end of their range are those arriving at the absorber with approximately 0.4 Bev kinetic energy. Protons responsible for the production of low energy stars must have energies of the order of several hundred Mev after traversing the lead absorber, since most of the stars which give rise to ionization pulses are probably produced in the walls or the gas of the chamber. The energy of these protons before traversing the absorber is of the order of 0.5 Bev. (Protons incident upon 15 cm of lead with energies between 0.4 and 0.6 Bev emerge from the lead with energies between 0 and 350 Mev.) One thus concludes that the protons detected by the anticoincidences $AI-B$ have a minimum energy of about 0.4 Bev and probably an average energy of the same order of magnitude.

Events in which all of the A trays fail to be discharged (anticoincidences $IB-A$) are interpreted as nuclear events initiated mostly by neutrons, but in small part by protons which miss the A trays. One might expect *a priori* that the average energy of the particles responsible for $IB-A$ events is somewhat lower than that of the particles responsible for AIB events. In fact, it is reasonable to assume that the ratio of neutrons to protons increases as the energy decreases because the low energy end of the proton spectrum is depleted by ionization loss. On the other hand, the distributions of AIB and $IB-A$ events according to pulse shapes do not show any significant difference (see Table III).

In agreement with the observations of Bridge and Rossi the present experiments show a fairly large proportion of cases in which more than one tray per event is discharged among those covering the lead shield. In the experiment of Bridge and Rossi events of this type were found to be caused in approximately equal numbers by nuclear interactions projecting ionizing particles upwards and by air showers. The contribution of air showers should be much smaller in our experiments than in those of Bridge and Rossi because of the more complete shielding of the ionization chamber. This conclusion is borne out by measurements taken with tray A_5 moved some distance away from the rest of the equipment. During these measurements we observed only three AIB events involving the discharge of tray A_5 and of one additional A tray against 34 similar multiple events involving the discharge of tray A_1. Figure 6 shows that the proportion of multiple discharges of the A tray is much greater for the AIB than for the $AI-B$ events. This may be taken as additional evidence for the greater energy of the particles involved in events of the AIB type. In fact, cloud-chamber pictures show that nuclear events of increasing complexity have an increasing probability of projecting secondary particles in backward directions.

The primary purpose of the experiment described was a study of the latitude and altitude dependence of the various events (see Table II). Consider first the result concerning AIB events. The absorption thickness obtained at 55°N for these events (125±8 g cm^{-2}) does not differ significantly from that obtained by other authors for high energy nuclear interactions.[4,9] The absorption thickness at 20°N (135±11 g cm^{-2}) seems to be somewhat greater than that at 55°N but the difference is not outside of the statistical errors. At the 300 g cm^{-2} depth the intensity ratio between 55°N and 20°N is 1.17±0.04. This small latitude effect is consistent with our previous conclusion concerning the energy of the protons selected by the *AIB* coincidences. The geomagnetic cut-off for primary protons[10] is about 1.0 Bev at 55°N and 12 Bev at 20°N. The latter value is only twice the energy estimated to be the minimum necessary for the production of an *AIB* event. It is interesting to note that the latitude effect for *AIB* events found in the present experiment is not very different from the latitude effect for penetrating showers found by Walsh and Piccioni[11] between the same two latitudes (1.11±0.019).

The altitude dependence of the *AI–B* events at 55°N is not significantly different from that of the *AIB* events. There is an indication of an increase of the absorption thickness of *AI–B* events with decreasing latitude but the effect is not outside the experimental errors which, in this case, are very large. The intensity ratio between 55°N and 20°N at the depth of 300 g cm^{-2} amounts to 1.96±0.18 and is thus greater than the corresponding ratio for the *AIB* events. According to our previous discussion, most of the *AI–B* events are due to protons of energy not much greater than 0.4 Bev. The intensity ratio for these protons may be compared with the effect found by Conversi[12] for protons of approximately 15 cm Pb range (0.4 Bev energy) which amounts to about 2.1 between the latitude of 55°N and 20°N.

Events *IB–A*, which, according to our interpretation, are mainly due to high energy neutrons, have possibly a somewhat greater absorption thickness than events *AIB*. Their latitude effect (1.32±0.05) seems to be intermediate between those of the *AIB* and *AI–B* events.

For the discussion of the zenith angle dependence, consider that if there were no change of direction in the propagation of the nucleonic component through the atmosphere, the intensity $I(x, \theta)$ of this component at the depth x and the zenith angle θ would equal the vertical intensity at the depth $x/\cos\theta$. Under this assumption and with an exponential function, $\exp(x/L)$, to represent the dependence of the vertical intensity on depth, one obtains for $I(x, \theta)$ the expression

$$I(x, \theta) = I(x, 0)e^{-x/L[(1/\cos\theta)-1]}. \quad (1)$$

[9] J. Tinlot, Phys. Rev. **73**, 1476 (1948); **74**, 1197 (1948).
[10] M. S. Vallarta, Phys. Rev. **74**, 1837 (1948).
[11] T. G. Walsh and O. Piccioni, Echo Lake Conference on Cosmic Rays, 1949.
[12] M. Conversi, Phys. Rev. **76**, 444 (1949).

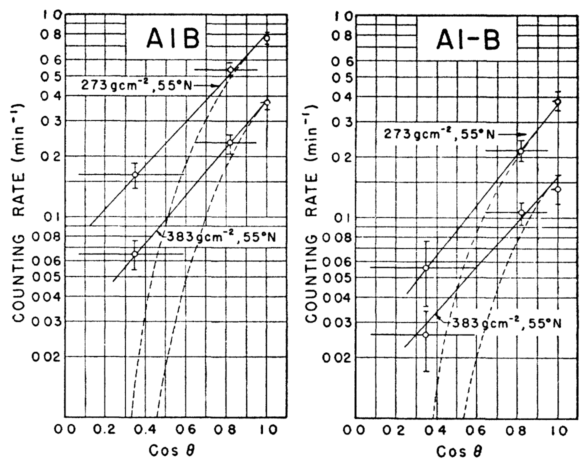

FIG. 7. Angular dependence of *AIB* and *AI–B* events observed at 55°N.

The dotted lines in Fig. 7 represent the angular dependence computed from Eq. (1) with $L = 125$ g cm^{-2}. One sees that whereas the observations at $\theta = 0$ and $\theta = 35°$ are not inconsistent with the law expressed by Eq. (1), the observations at $\theta = 70°$ indicate much greater intensities than one would anticipate according to this law. The observed discrepancies cannot be explained by the poor geometric resolution of the equipment. Nor can they be explained by an angular selectivity of the detector due to the fact that tray *B* is more likely to be discharged by the nuclear interactions of rays coming at a small zenith angle. This selectivity tends to increase the relative number of *AI–B* events observed at large zenith angles, but has the opposite effect on *AIB* events. It thus seems necessary to conclude that most of the nucleons observed at large zenith angles are the products of nuclear interactions occurring in the atmosphere above the instrument and in which high energy nucleons are emitted at wide angles to the direction of the primary particle.

The data on the E–W effect, unfortunately, was affected by large statistical errors. It is certain, however, that even at 20°N the asymmetry, if it exists at all, is small for both *AIB* and *AI–B* events. This may be due, at least in part, to a loss of directionality in the propagation of high energy nucleons through the atmosphere, such as is indicated by the measurements on the zenith angle dependence.

We wish to thank Herbert Bridge of the M. I. T. staff and William A. Higinbotham of the Brookhaven National Laboratory for advice and help in constructing the electronic equipment; the Air Materiel Command, United States Air Force, and to thank in particular the personnel of the 3171st Electronics Research Group. Rome, New York, who flew the B-29 airplane.

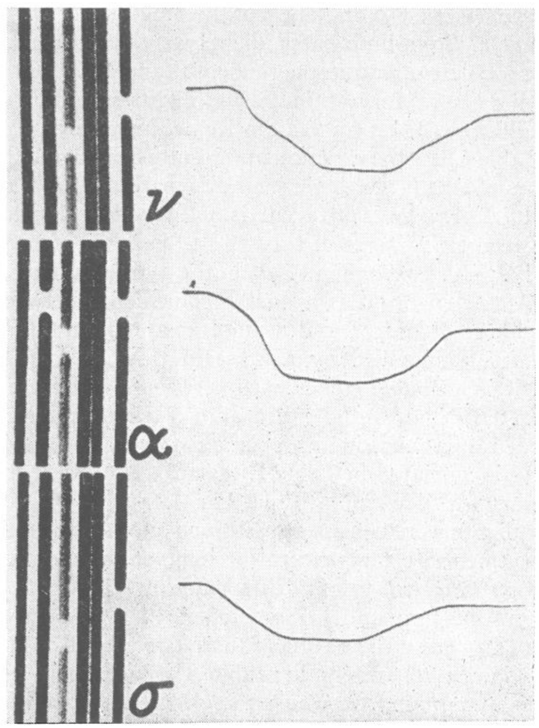

FIG. 4. Samples of photographic records showing a ν-pulse, an α-pulse, and a σ-pulse. The black lines on the left-hand side represent the images on continuous moving film of the neon bulbs recording discharges of the counter trays.